EuroCirCol A key to New Physics

FCC H2020 Project

CERN

Status FCC CDR

R. Kersevan

(input courtesy of F. Zimmermann, M. Benedikt, CERN)

FCC-CDR Progress

Dashboard progress weekly report 5/10/2018

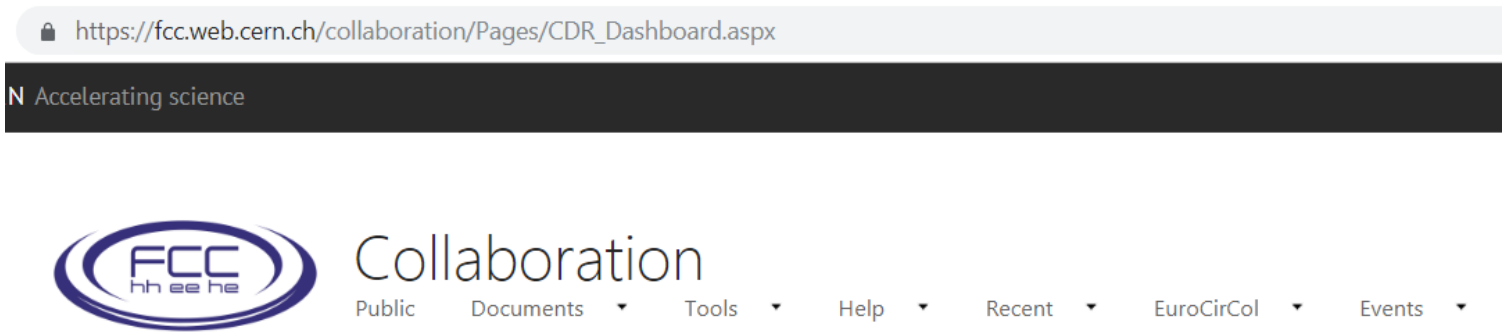

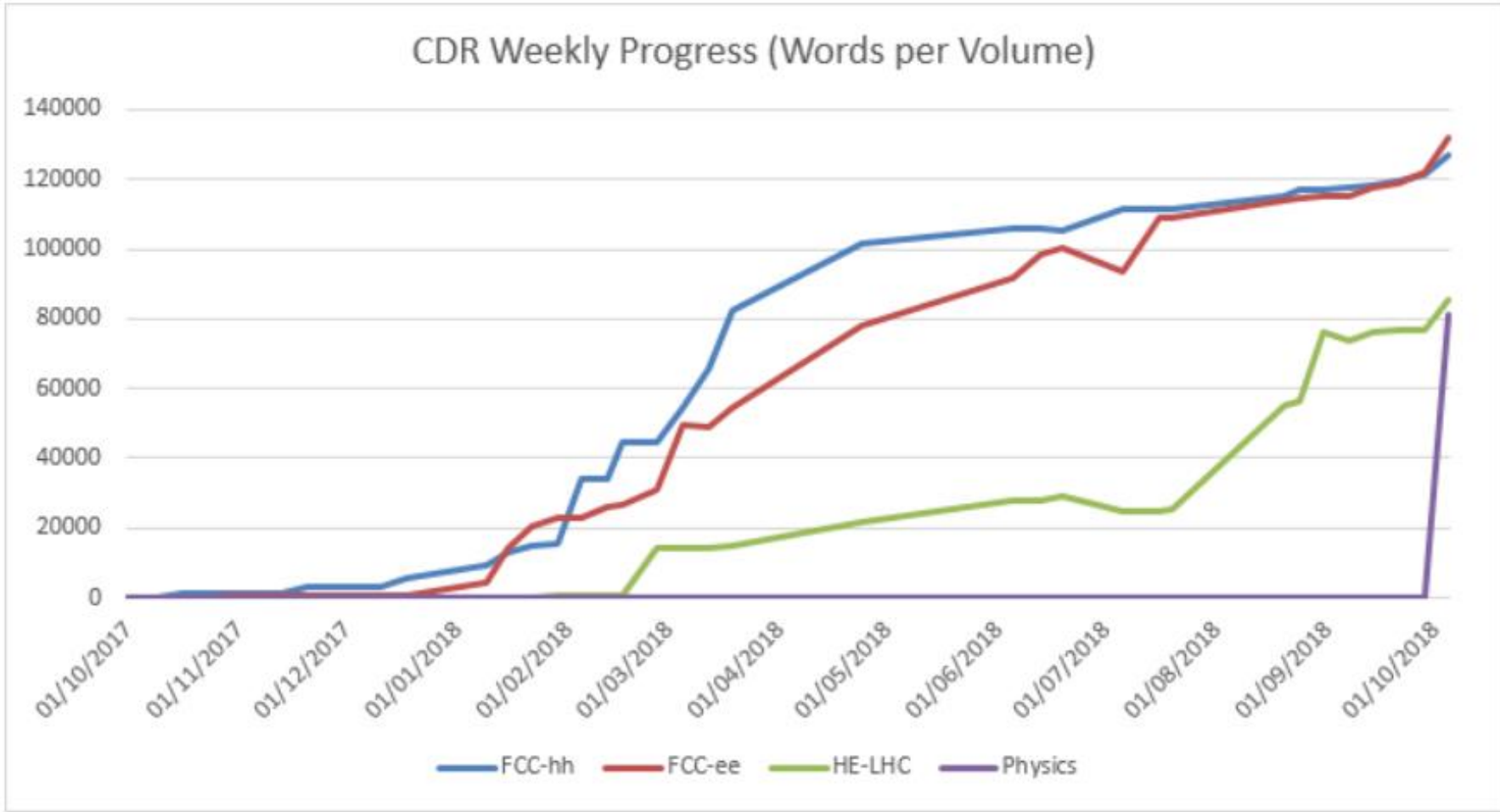
CDR Weekly Progress (Words per Volume)
140000
120000
100000
80000
60000
40000
20000
0
01/10/2017
01/11/2017
01/12/2017
01/01/2018
01/02/2018
01/03/2018
01/04/2018
01/05/2018
01/06/2018
01/07/2018
01/08/2018
01/09/2018
01/10/2018
FCC-hh
FCC-ee
HE-LHC
Physics

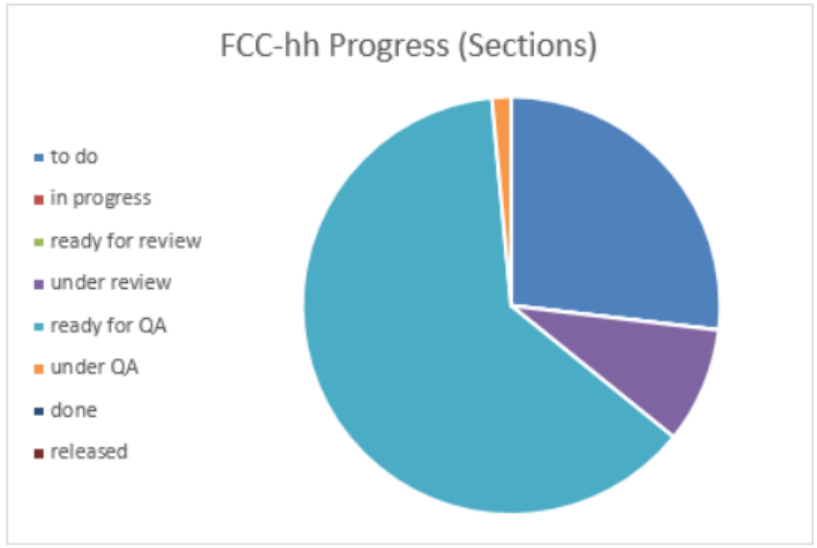
FCC-hh Progress (Sections)
to do
in progress
ready for review
under review
ready for QA
under QA
done
released

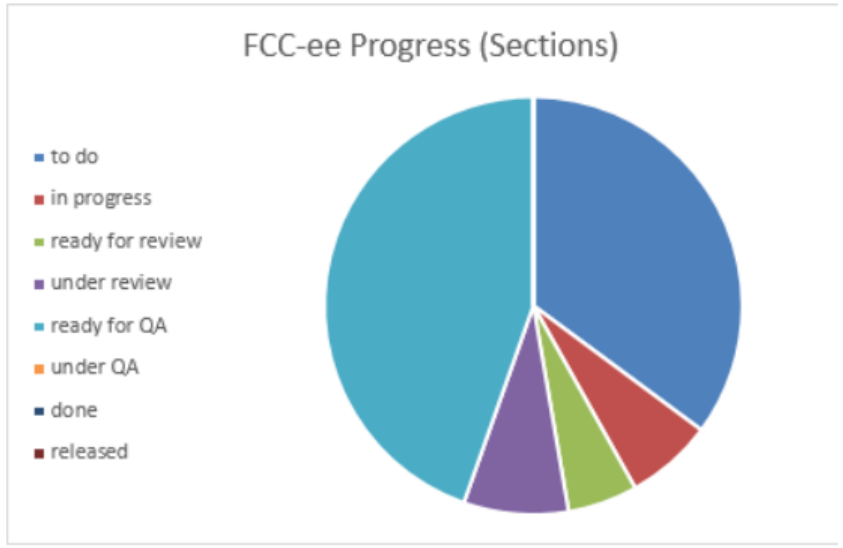
FCC-ee Progress (Sections)
to do
in progress
ready for review
under review
ready for QA
under QA
done
released

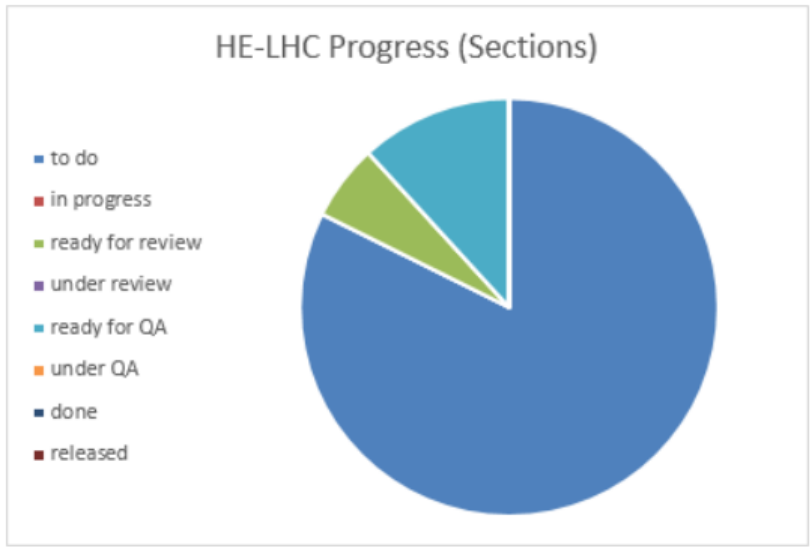
HE-LHC Progress (Sections)
to do
in progress
ready for review
under review
ready for QA
under QA
done
released

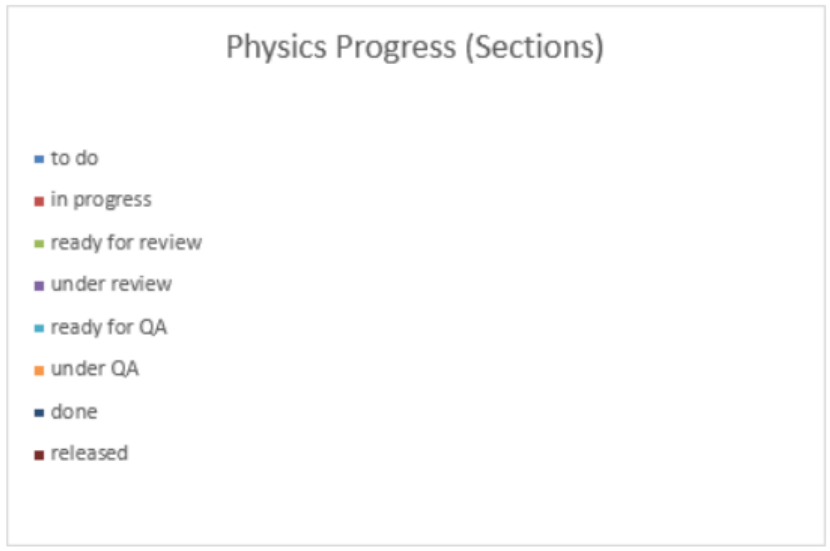
Physics Progress (Sections)
to do
in progress
ready for review
under review
ready for QA
under QA
done
released

From M. Benedikt presentation

CDR progress

- **The volumes have been renumbered:**
  - Physics: Vol 1
  - FCC-ee: Vol 2
  - FCC-hh: Vol 3
  - HE-L
- **Planning for finalisation:**
  - Vol 2 FCC-ee: frozen by Sunday 30 September
  - Vol 3 FCC-hh: frozen by Sunday 14 October
  - Vol 1 Physics: frozen by Sunday 21 October
  - Vol 4 HE LHC: frozen by Sunday 21 October

From M. Benedikt presentation

CDR progress

- **Author list for CDR:**
  - 30 October invitation to sign up as CDR authors
  - Registration will finish on 10 November
  - Possibly we will put a link to the inspire institution database for selection of affiliation

- **All 4 CDRs must be ready for printing end November to be distributed from December 10 (Council week)**

- **10-page documents:**
  - One document per machine option: FCC-ee, FCC-hh and HE-LHC
  - One document on staged implementation, FCC-ee followed by FCC-hh with option of eh. This should show the robustness of the overall approach and also the flexibility to adapt.
  - In total 4 of the 10-page documents are planned at this stage.
  - Deadline Sunday 11 November, to allow iteration with directorate.

Future Circular Collider Study
Volume 3 - The Hadron Collider (FCC-hh)
Conceptual Design Report

CONFIDENTIAL DRAFT
V0.24, 3.10.2018
DO NOT DISTRIBUTE

2.3.2 Arc Vacuum

The arc vacuum system defines the aperture of the magnet, which is a key cost driver and has a strong impact on the beam performance. The proposed design allows the magnet aperture to be reduced to 50 mm and still provides good conditions for the beam, i.e. good vacuum, low impedance and suppression of electron cloud effects.

The beamscreen protects the cold bore of the magnets from the 30 W/m of synchrotron radiation emitted by each beam at collision energy (see Section 3.3.2). The cryogenic system cools this screen to 50 K at which temperature it is much more efficient for the removal of the heat than the 2 K system of the magnets.

A vacuum pressure of 10^{15} m^{-3} hydrogen equivalent, similar to the LHC, ensures a beam lifetime of about 100 hours, which is compatible with the integrated luminosity target. The power deposited by beam scattering on the rest gas is low enough to avoid quenches of the superconducting magnets due to induced heating. However, with this lifetime up to about 40 kW (0.45ÃŠ,W/m) is still being deposited in the arc dipoles and removal of this requires about 30 MW of cooling power. Therefore the vacuum design is aimed at a significantly lower vacuum pressure of 0.2×10^{15} m^{-3} hydrogen, which is feasible.

The copper coating of the inner surface of the beamscreen in combination with the chosen aperture ensures that the impedance is low enough for beam stability, although a high-temperature superconductor (HTS) coating option is being considered to provide a higher stability margin. Pumping holes in the screen facilitate a good vacuum and in contrast to the LHC, they do not generate significant impedance because they are located in two small antechambers. The antechambers also help to reduce the amount of synchrotron radiation that is reflected back into the beam aperture. This arrangement reduces the production of seed electrons that could form an electron cloud. A thin coating of amorphous carbon on the inner part of the chamber hinders any existing electrons from producing electron showers thereby suppressing any electron cloud build-up.

Future Circular Collider Study
Volume 3 - The Hadron Collider (FCC-hh)
Conceptual Design Report

CONFIDENTIAL DRAFT
V0.24, 3.10.2018
DO NOT DISTRIBUTE

3.3 Cryogenic Beam Vacuum System

3.3.1 Overview

Vacuum stability at cryogenic temperature is a key element for the desig
icant levels of synchrotron radiation are produced in this machine that
in the order of 30 W/m. Early analysis has revealed that it is unlikely to
akin to the one in the LHC that can cope with the operation conditions
can effectively shield the cold bore of the superconducting magnets o
load. The concept must also help mitigating electron cloud, resistive
beginning. The proposed design is currently being experimentally vali
that it can keep the heat load below 300 mW/m.

3.3.2 Beamscreen

3.3.2.1 Synchrotron radiation, impedance and cryogenic considerations

The synchrotron radiation (SR) power and flux are higher than those of the LHC. Figure3.7 shows a comparison between the LHC, FCC-ee, and FCC-hh flux spectra from 4 eV to 1 MeV. A 4 eV cut-off has been chosen because photons below 4 eV, the typical value of work-function for metals, are incapable of extracting photo-electrons and producing molecular desorption from the walls of the beamscreen. While the linear photon flux for FCC-hh is only a factor of 3.5 times higher than that of LHC, the linear SR power density at 50 TeV is almost 200 times higher than that of the LHC, ruling out a scaled version of the LHC beamscreen. Calculations [158] have ruled out the possibility of using LHC sized capillaries (<4 mm) because the supercritical helium flow rate would not be sufficient. The required number of pumping slots would also affect the impedance budget too much [159]. For these reasons the design concept foresees longitudinal slots along the external part of the beamscreen in the plane of the orbit, where the highly collimated SR photon fan is directed.

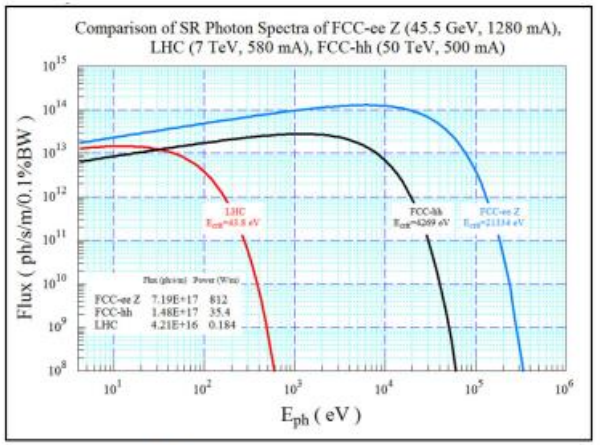

Figure 3.7: Comparison of the SR flux spectra for LHC, FCC-ee (Z-pole) and FCC-hh.

3.3.2.2 Beamscreen design

Figure 3.8 shows the beamscreen design concept. With respect to initial designs, the height of the two longitudinal slots has been increased to limit effects on the impedance budget. This improvement is also beneficial for vacuum quality, since it captures a larger fraction of the primary SR photon fan during the acceleration phase. At lower beam energies the rms vertical aperture of the SR photon fan is bigger, as it depends on the reciprocal of the relativistic factor [160]. The number and position of the pumping slots has been optimised taking into account the leakage of scattered SR power reaching the magnet cold-bore. The internal surface of the beamscreen would be treated using Laser-Ablated Surface Engineering (LASE), creating μm sized patterns on the surface. This treatment has proved [161] to greatly reduce the secondary-electron yield (SEY) of the bare surface. Experimental validation of LASE treated surfaces on the resistive wall impedance to reduce SEY and photo-desorption yield are ongoing in the EC funded EuroCirCol project [161]. Details of the measurements on 3 variations of the beamscreen will be reported at the 2018 FCC week [162]. If HTS coatings are chosen for improved impedance reduction, e-cloud mitigation would be provided by an a-C coating.

Future Circular Collider Study
Volume 3 - The Hadron Collider (FCC-hh)
Conceptual Design Report

CONFIDENTIAL DRAFT
V0.24, 3.10.2018
DO NOT DISTRIBUTE

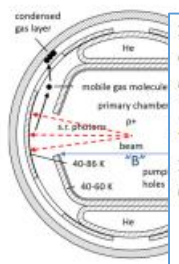

Figure 3.8: : Latest design of the
indicated with details of the tempera
width "B" of 27.55 mm. The large p
beamscreen of ~860 l/m/s at 50 K (
the copper layer on the inside of the
80 μm.

3.3.2.3 *Beamscreen temperature*

The total SR load is ~2.3 MW/beam
ature between 5 K (inlet) and 20 K (
cryo-compressor electric power inpu
sible to operate [158]. A detailed a
for the beamscreen for a workable sy
outlet of each cell should be betwee
timum working point for a cryogeni
resistivity of Cu [163] and also idea
range is also advantageous for the
tional to the square root of the absolu
instability is excited [165].

3.3.2.4 *Heat load to cold bore*

Table 3.9 gives an overview of all
mounted using elastic springs in the
results show that the total heat load i

Tab

SOURCE	
Beam-gas scattering	
Thermal conduction	
Grey body thermal ra	
Leaked radiation pow	
Total heat load	

3.3.2.5 *Residual gas density*

The requirements in terms of residu
acceptable level was specified for an

nuclear scattering lifetime, i.e. a gas density of a mixture of gases usually released by SR irradiation, consisting of H_2, CO, CO_2, CH_4, each weighted with its radiation length and percentage molecular content and referred to that of 100% H_2 [168]. A scaling has been performed for a hadron beam at 50 TeV [2]. Given the higher beam energy and the less-than-linear increase of the nuclear scattering cross-section with beam energy, it has been estimated that ~5 times the required decrease of H_2-equivalent density is needed to achieve the same 100 hour lifetime contribution. The target is to remain below 2×10^{14} H_2-equivalent m^{-3}.

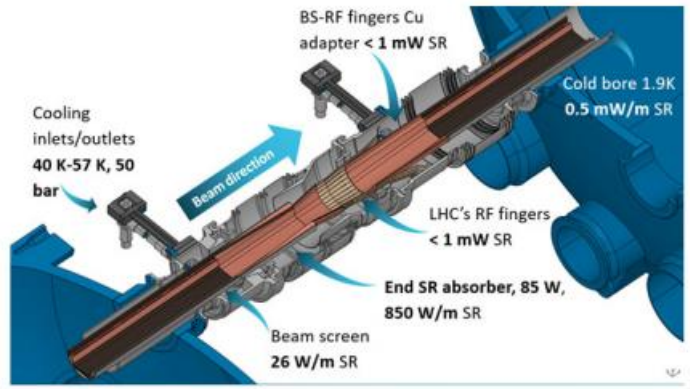

Figure 3.9: Cut-through, in the plane of the orbit, of the dipole-to-dipole short interconnect area model. This model does not show the BPM block, which is under design in another work package.

A 3D CAD model of the arc dipole and interconnect area has been created [168] based on the LHC. It takes into account the new requirements, SR photon flux and linear power densities. It has been found that the RF fingers installed after each dipole and quadrupole, compensating displacements and thermal contraction during cool-down, need to be shielded from the primary SR photon fan. Otherwise be damaged as a result of the 35 W/m power density. A symmetric SR absorber upstream of the RF contact fingers, as used in modern light sources, mitigates that risk. The absorber intercepts and concentrates up to 85 W of SR power, casting a shadow downstream for about 2–3 m, up to the subsequent beam screen. Along the shadowed area, the racetrack shaped beam screen gradually merges into the circular shape which is needed for the LHC-style RF contact fingers and, eventually, for the beam-position monitor (BPM) button blocks.

Figure 3.9 shows a cut-away view of the interconnect area. Figure 3.10 shows a residual gas density profile generated by the SR fan after a conditioning time. At each point along the beam screen, the molecular desorption rate depends on the locally accumulated photon dose. This means that one always has to specify for which photon dose a pressure or density profile is being calculated. The photon dose at each point along the beam screen is calculated using 3D ray-tracing Monte Carlo simulation that has been validated with experimental data [168].

3.3.2.6 *Electron cloud mitigation*

There are a number of different proposals for electron cloud mitigation. One path currently being considered is using amorphous carbon (aC) coating, which has been successfully tested in the SPS at CERN. Another option is LASE treatment (see Fig. 3.8), which is also being assessed experimentally. Figure 3.11 shows the areas which would need to be treated, the corresponding percentage of copper-coated beam screen area and the electron cloud distribution for each type of magnetic element: dipole, quadrupole and field-free drift [169].

Future Circular Collider Study
Volume 3 - The Hadron Collider (FCC-hh)
Conceptual Design Report

CONFIDENTIAL DRAFT
V0.24, 3.10.2018
DO NOT DISTRIBUTE

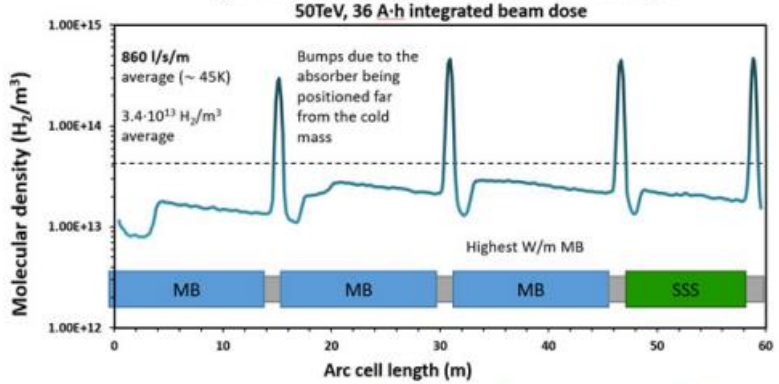

Figure 3.10: H_2 partial pressure profile for one full arc cell. All of the H_2 is due to SR, assuming that the static outgassing and the e-cloud contributions are negligible. The density spikes visible in the plot are located at the photon absorber positions, followed by shallow density minima corresponding to the shadowing of the absorbers and reduced photo-desorption.

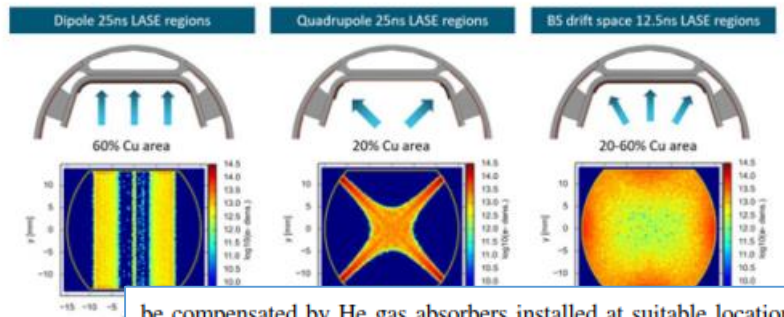

Figure 3.11: Cut-aw
model does not show

3.3.3 Vacuum

3.3.3.1 Insulation v

The insulation vacuu
distribution lines. The
fully for more than te
the large volumes, sta
installed at the vacuu
evacuate helium gas i

Equipping the a
to the cost of pumps,
pumping groups wou
reduced effective pur

be compensated by He gas absorbers installed at suitable locations and cooled to the lowest possible temperature. Other gas species are absorbed efficiently by the cold walls. The permanent turbo-molecular groups will also guarantee pumping during thermal transients of the cryostat which lead to excessive gas release from the absorbers.

3.3.3.2 Helium absorbers

The absorber material, its shape and its assembly in the cryostat are under investigation. The current conceptual design is based on compacted nano-porous materials fixed in thermal contact with the cold-mass support cooling pipes at 4.5 K (the C' line in LHC terminology).

The development of the He absorbers can benefit from the large spectrum of studies performed over the last ten years, in particular for the ITER project [159, 163, 168]. He pumping has been measured for activated charcoal fixed on metallic surfaces. Surface areas available for absorption regularly exceed 3000 m^2 per gram of absorber; this means that 30 g of activated charcoal would have the same surface area available as the total multi-layer insulation (MLI) in a 400-m long vacuum sector. In the coming years, the focus will be to develop a material with a well defined porous structure for He pumping at affordable cost for quantities around ~100 kg. The activation of the absorbers in the cryostats also currently under investigation.

Future Circular Collider Study
Volume 2 - The Lepton Collider (FCC-ee)
Conceptual Design Report

CONFIDENTIAL DRAFT
V0.11, 3.10.2018
DO NOT DISTRIBUTE

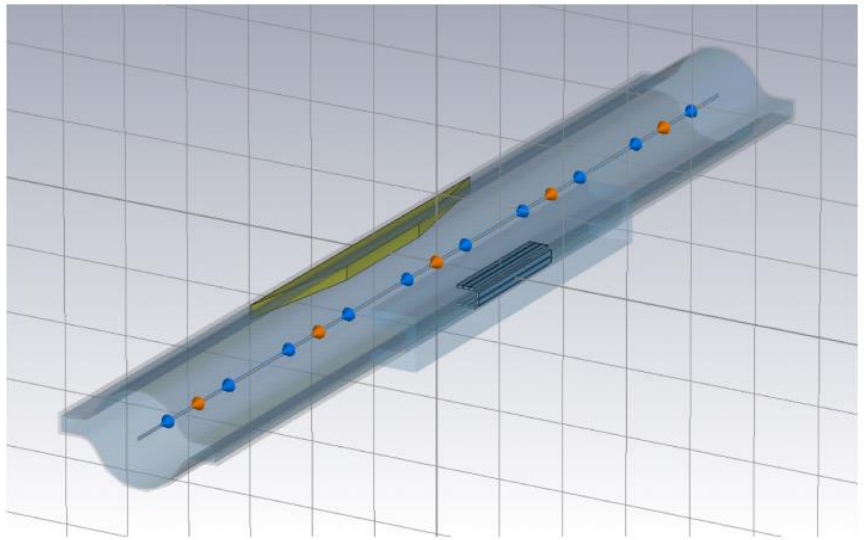

Figure 2.17: 3D model of the FCC-ee chamber and an SR absorber with pumping slots used for CST simulations.

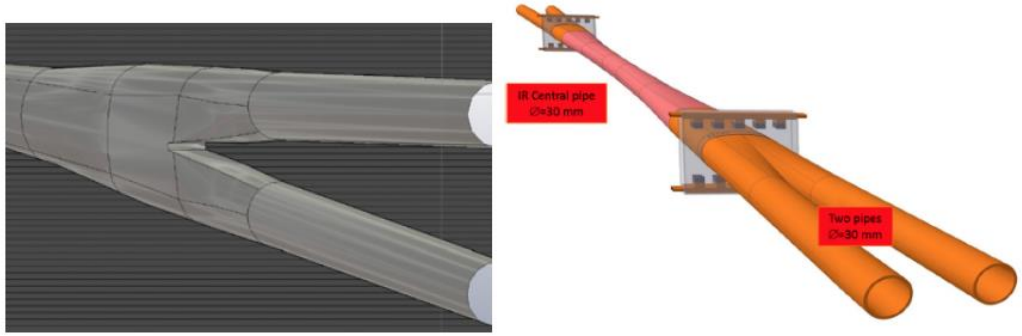

Figure 2.13: Left: 3D CAD view of the IR vacuum chamber in the region where two beam pipes merge; Right: beam pipe with HOM absorbers.

Future Circular Collider Study
Volume 2 - The Lepton Collider (FCC-ee)
Conceptual Design Report

CONFIDENTIAL DRAFT
V0.11, 3.10.2018
DO NOT DISTRIBUTE

3.3 Vacuum System and Electron-Cloud Mitigation

3.3.1 Introduction

The FCC-ee, with the same total synchrotron radiation (SR) power budget of 50 MW/beam for beam energies ranging from 44 to 182.5 GeV, is a challenging machine from the point of view of the design of its vacuum system. Naively one could think of designing it by copying the LEP vacuum system, which was run in its latest versions above 100 GeV. Close scrutiny of the technical parameters of LEP and FCC-ee demonstrate that such an approach is not warranted. First, LEP had a single-beam design, with both beams circulating inside the same chamber, while FCC-ee calls for two separate beams. Secondly, the FCC-ee lowest-energy versions at 44 – 47 GeV (Z-pole), feature an extremely "B-factory-like", current of almost 1400 mA. This specification together with the operation scheme that allocates the first 4 years to the study of the Z-pole resonance with an aggressive integrated luminosity goal, calls for a radically different design of the vacuum system. Furthermore, the same vacuum system must also be compatible with the higher beam energy of up to 182.5 GeV (above the $t\bar{t}$ threshold), with its attendant very high critical energy SR spectrum (~1.2 MeV for arc dipoles), as well as the intermediate beam energies of 80 GeV (WW threshold) and 120 GeV (ZH production). A summary description of the proposed vacuum system, based on extensive Monte Carlo simulation ray-tracing and modelling (SYNRAD+, Molflow+) and finite-element analysis (Comsol, ANSYS), is given in the following sections.

3.3.2 Arc Vacuum System

3.3.2.1 Vacuum chamber material and cross-section

The SR fan generated by the arc dipoles can be absorbed on the vacuum chamber in two ways, namely a distributed absorber (as in LEP) or by a series of localised absorbers (as is done in light sources). The advantage of the first option is that it is easy to extrude a vacuum chamber with an integrated cooling water channel in aluminium alloys. A similar design has also been implemented in vacuum chambers made from copper alloys, although the cooling water circuit must be welded onto the chamber, as there is no way to extrude convoluted geometries in copper. It has been demonstrated in FLUKA simulations [271] that the use of aluminium alloys is not possible in FCC-ee. This is because there is a considerable quantity of SR photons generated above the Compton edge energy (around 100 keV), at beam energies around and above the W-pole. For aluminium chambers, SR photons of this energy cause radiation leakage from the vacuum chamber which becomes an issue in terms of radiation protection, material activation and damage to nearby components.

Copper, which is a better photon absorber than aluminium, has been chosen as the material and the design localises the absorption of the SR fans on a finite number of water-cooled photon absorbers, as is done routinely at modern light sources. This design has a two-fold advantage, namely: 1) it concentrates the SR fan on a small surface (one absorber of ~150 mm length can intercept the photons which would otherwise be distributed over 4-5 metres of vacuum chamber wall) and this speeds up the dynamic vacuum conditioning, which depends, to a first approximation, on the linear photon density along the beam axis; 2) localised absorbers allow the installation of local high-atomic number shielding (like Pb or W alloys), thus avoiding the need for complete cladding of the vacuum chamber system, as was done for LEP (this later proved to be a source of problems during operation, namely the depolarisation of the beams due to the thin nickel layer between the aluminium chamber and the lead cladding). The absorbers are placed strategically to intercept 100% of the primary SR fans. The total power intercepted by each absorber varies between 4 and 7 kW, depending on the location in the arc lattice. This is a typical value for SR absorbers at many of today's light sources, so it is assumed that it is a reasonable and proven design assumption for FCC-ee.

Summarising, the aim is to design a copper alloy vacuum chamber with a suitable number of localised, short, water-cooled photon absorbers.

An additional important technical requirement is that the vacuum chamber shape should be as close as possible to circular, since an elliptical chamber results in an unacceptable impedance [272]. Taking all these requirements into account, the proposed cross section of the vacuum chamber in the arcs is derived from the SuperKEKB collider chamber, i.e. a circular tube with two "winglets" placed symmetrically in the plane of the orbit, 20 mm wide and 11 mm tall. For FCC-ee, the round part of the chamber cross-section has a diameter of 70 mm, corresponding to a specific conductance of about 42 l×m/s (compared to the ~100 l×m/s of the LEP elliptical chamber).

The winglet on the external side, i.e. where the SR fan goes, is used to lodge the localised photon absorbers, which have a tapered surface which does not protrude into the round part of the chamber where the e^-e^+ beams circulate. The absorber design is rather compact, only ~ 300 mm in length, and

Future Circular Collider Study
Volume 2 - The Lepton Collider (FCC-ee)
Conceptual Design Report

CONFIDENTIAL DRAFT
V0.11, 3.10.2018
DO NOT DISTRIBUTE

11 mm tall.

Detailed finite-element calculations have shown that a 2 mm thick vacuum chamber wall is sufficient to guarantee thermo-mechanical stability during both operation and bake-out (at ~ 200°C).

The SuperKEKB design allows the implemention of a continuous cross-section, without tapered transitions, along most of the arcs. This in contact fingers inside the bellows. The latte during operation and bake-out (and even t chamber supports due, for example, to tunne

As in SuperKEKB, rectangular flang quadrupole and inside the dipole-yoke ope regular circular ConFlat flanges. The Super and "hard" copper flanges of this design, wh ing.

The vacuum chambers are straight ev at a small angle to each other, an angle whi alignment in the tunnel. The ~2 mm sagit accommodated inside a straight chamber of

Another important feature of the abso and a suitably "large" pumping speed can be trapping efficiency of the pumps, which in t vacuum-related beam lifetime must be long scattering) which translates, for the high-cu ditioning to achieve low SR-induced desorp implemented next to each photon absorber. a flat rectangular connection with RF shieldi any trapping of high-order modes.

Two different designs are required f one for the chamber placed externally with internally. The need for two designs become dome can be placed opposite a photon abso the pumping dome must be placed on the sa (or quadrupole) does not leave enough space FLUKA simulations indicate that it is better photon absorber.

3.3.2.2 *Vacuum system pumping*

The aggressive integrated luminosity target pole beam energy calls for a design which g with the additional requirement of a sufficien in order to minimise and possibly avoid any

Taking the positive behaviour of the and the fact that many SR light sources hav ogy since the year 2000, a complete coating However, a "standard" 1–2 µm thick NEG la budget of the FCC-ee [273]. An alternative thickness would be compatible with the RW solution. Laboratory measurements at CERN multiple activation/saturation cycles without

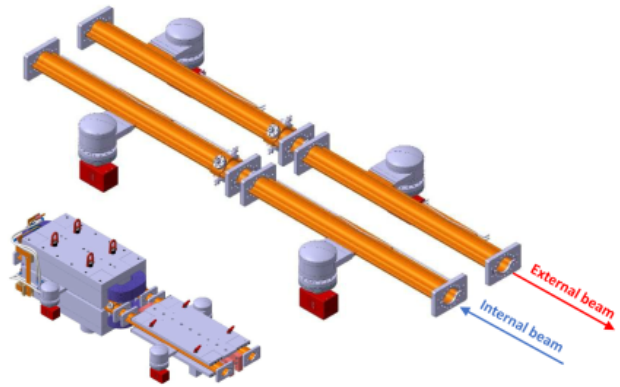

Figure 3.11: Schematic of the FCC-ee arc vacuum system. The small picture on the bottom left shows the same vacuum system inserted into a twin quadrupole (at the back) and a twin dipole magnet (in front).

test some tubes coated with these thin NEG films under SR irradiation at the KEK Photon Factory before the end of 2018. These tests will measure the SR-induced molecular desorption yield, which for standard thickness NEG-coatings have been shown to desorb ~100 times fewer molecules than an uncoated system of the same geometry [275].

It has been shown that the generation of CH_4 through SR-induced desorption mechanism is much reduced by the presence of NEG-coating: accordingly, a large pumping speed for such a non-getterable gas is not needed and, therefore, pumps of the NEXTorr family (SAES Getter Inc., Milan) will be installed in the pumping domes. NEXTorr pumps are based on NEG technology, using blades or discs of sintered NEG material and have an integrated ion-pump which has about 10 l/s pumping speed which should be sufficient to pump the non-getterable gases, such as CH_4 and Ar. As an alternative to the compact NEXTorr pumps, medium-sized sputter-ion pumps (e.g. 80–120 l/s) could be installed, or the two types of pumps could be alternated. The conductance of the pumping dome's rectangular slot and RF slotted shield has been calculated to be ~110 l/s, so that a 120 l/s nominal pumping speed would be reduced to about 1/2 of its value, which is deemed acceptable.

Another advantage of the NEG-pumps is that they do not need any permanent local high-power cabling, since the NEG part of the pump, which produces the bulk of the pumping, can be activated with local controllers manned during the bake-out cycle. The gas capacity for CO and CO_2 of a 500–1000 l/s NEXTorr pump is very large, meaning that the pump should not need re-activation other than during the scheduled shutdown periods of the accelerator, i.e. there will be no impact on the machine availability.

Given the very large radius of curvature of the arc dipoles (~11 km), the total length of the arcs, the two-chamber design and the fact that the distance between absorbers is of the order of 5 m, the total number of pumps, if placed in front or near each absorber, would be ~16000. In order to optimise the cost, MC simulations showing the effect on the average pressure for a reduced number of pumps, installing one pump every 3 or 5 absorbers have been made. The result is that the dynamic vacuum conditioning time, i.e. the integrated beam dose (Ampere-hour) before reaching a suitably low average value of the SR-induced desorption yield, is doubled. This reveals a fundamental limit dictated by the geometry of the system, mainly the aperture in the magnets and the radius of curvature of the dipoles.

Future Circular Collider Study
Volume 2 - The Lepton Collider (FCC-ee)
Conceptual Design Report

CONFIDENTIAL DRAFT
V0.11, 3.10.2018
DO NOT DISTRIBUTE

3.3.2.3 Bake-out and ancillary systems

Water vapour is always present on the surface of a chamber when it is installed in a tunnel and it needs to be removed. Depending on the material, molecules can be chemically and physicall the water vapour removal is to bake-out th 120-130 °C for times of at least 1 to a few pumps, typically): the higher the temperatu NEG-coatings, based on ternary ZrTiV allo activation, a system which is capable of sus

A suitable means of heating up the rent technology provides ceramic heaters w chamber at suitable locations, the high-the around the profile of the chamber. An insu temperature-sensitive components or devi jackets corresponding to this specification

The RF contact fingers are based o called "comb-type design" [276]. The exis same cross-section to be maintained all alo every flange connection. In addition, there only the long straight sections where the s where special devices will be installed (e.g require tapered transitions from the SuperK devices/components. The possibility of inte has already been demonstrated at the Supe that the low-emittance FCC-ee would need of the beam and its trajectory and therefore feature.

3.3.2.4 Vacuum chamber supports and a

The LEP arc had vacuum sectors of about ticality of having very long independent required at either end of every sector, mus detailed here.

The supports for the vacuum chamb but there do not appear to be any major issu given that most of the chambers along the copper chamber it would be of the order of thick SuperKEKB-type rectangular flanges be located at the flanges and, if necessary, can be aligned precisely, with respect to the which the cooling efficiency is optimised. support, possibly acting as a fixed point.

3.3.3 IR Vacuum System

For most of the FCC-ee straight sections t is similar to the arc system except that in magnets. The SuperKEKB-type chamber p is connected to a custom absorber, which pr

The ray-tracing Monte-Carlo code SYNRAD+ has been applied to the entire FCC-ee interaction regi was and pipe mas of k like redu with area high behi HO occu poss circ flux mos bey

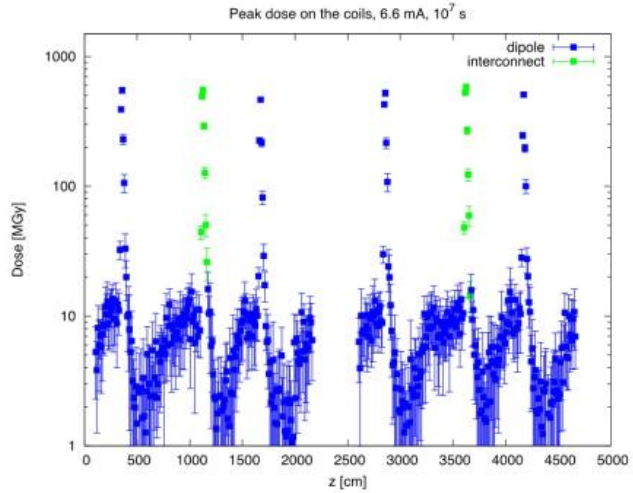

Figure 3.13: Peak annual dose profile in the arc dipole coils along a 50 m cell, for 6.6 mA beam current over 116 days per year at 175 GeV beam energy [280]. Maxima correspond to the absorber locations, with two absorbers sitting in the interconnect rather than inside the dipole. Vertical bars give the statistical error.

3.3. The of high-energy radiation generated by one ring onto the other, through primary and secondary showers, and by either ring onto the tunnel wall and other components/devices placed inside the tunnel. See also Section 3.12.

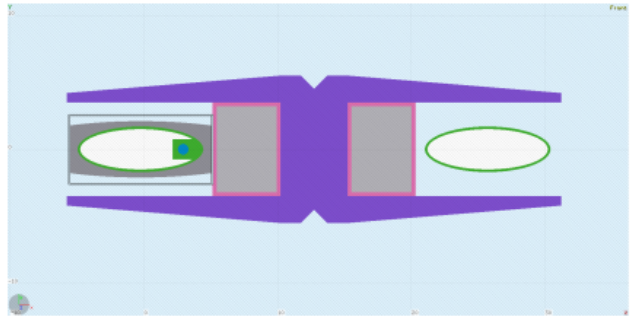

Figure 3.12: Arc dipole transverse section, as implemented in a preliminary FLUKA model, featuring on the inner (left) side a photon absorber (in green) surrounded by lead shielding (in grey) [280].

To minimise the impact of this radiation, adequate shielding of the arc vacuum chamber is particularly important for the higher-energy working points (H, $t\bar{t}$), with critical photon energies extending up to

Future Circular Collider Study
Volume 4 - The High Energy LHC (HE-LHC)
Conceptual Design Report

CONFIDENTIAL DRAFT
V0.7, 3.10.2018
DO NOT DISTRIBUTE

2.3.1 Synchrotron Radiation

Table 2.2: Synchrotron radiation (SR) characteristics in the arcs of LHC, HE-LHC and FCC-hh.

Parameter	LHC	HE-LHC	FCC-hh
Linear SR power [W/m]	0.25	5.5	35
Linear photon flux [10^{16} photons/m/s]	5	27	15
Critical photon energy [eV]	44	320	4300

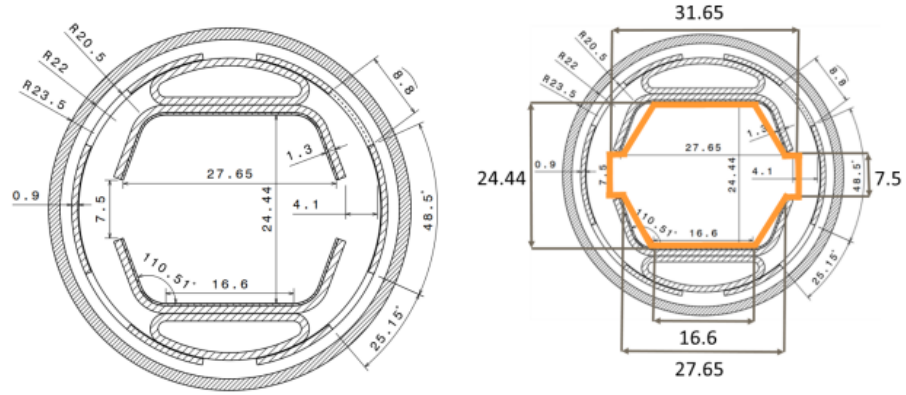

Figure 2.1: Beamscreen proposed for FCC-hh and HE-LHC [16] (left picture) and approximation used for aperture calculation [17] (orange line, right picture).

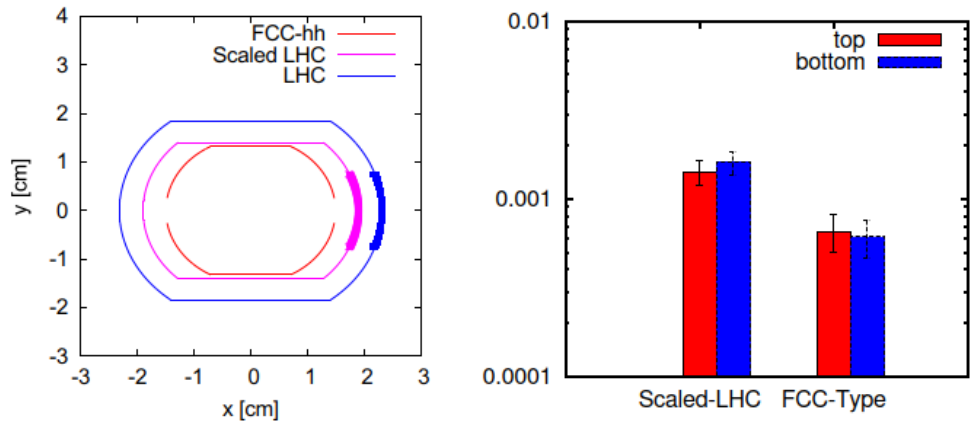

Figure 2.2: Left: Vacuum chamber cross sections for FCC-hh, LHC and scaled LHC beamscreens, where the thicker line represents the sawtooth on the wall and transparent region is an opening slot. Right: The fraction of photons absorbed with a 95% confidence interval at the top and bottom of the two vacuum chambers proposed for the HE-LHC [18].

Future Circular Collider Study
Volume 4 - The High Energy LHC (HE-LHC)
Conceptual Design Report

CONFIDENTIAL DRAFT
V0.7, 3.10.2018
DO NOT DISTRIBUTE

3.3 Cryogenic Beam Vacuum System

3.3.1 Overview

Vacuum stability at cryogenic temperature is a key element for the des
levels of synchrotron radiation are produced in this machine that result
order of 5 W/m. Early analysis has revealed that it is unlikely to be poss
to the one in the LHC that can cope with the expected operation condi
that can effectively shield the cold bore of the superconducting magnets
load. The concept must also help mitigating electron cloud, resistive
beginning. The proposed design is currently being validated experiment

3.3.2 Beamscreen

3.3.2.1 Synchrotron radiation, impedance and cryogenic considerations

The synchrotron radiation (SR) power and flux are higher than those of the LHC. Figure 3.6 shows a comparison between the LHC, HE-LHC, and FCC-hh flux spectra from 4 eV to 1 MeV. A 4 eV cut-off has been chosen because photons below 4 eV, the typical value of work-function for metals, are incapable of extracting photo-electrons and producing molecular desorption from the walls of the beamscreen. While the linear photon flux for HE-LHC is only a factor of 4 times higher than that of the LHC, the linear SR power density at 13.5 TeV is about 30 times higher than that of the LHC, ruling out a scaled version of the LHC beamscreen. Calculations [101] have also ruled out the possibility of using LHC sized capillaries (<4 mm) because the supercritical helium flow rate would not be sufficient. The required number of pumping slots would also affect the impedance budget too much [102]. For these reasons the design concept foresees longitudinal slots along the external part of the beamscreen in the plane of the orbit, where the highly collimated SR photon fan is directed.

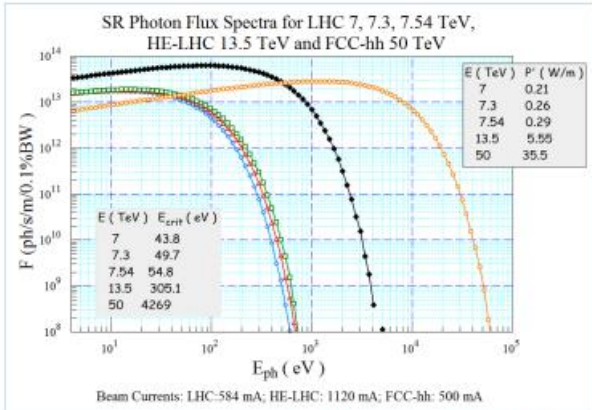

Figure 3.6: Comparison of the SR flux spectra for LHC at three energies, HE-LHC and FCC-hh.

3.3.2.2 Beamscreen design

Figure 3.7 shows the beamscreen design concept. With respect to initial designs, the height of the two longitudinal slots has been increased to limit effects on the impedance budget. This improvement is also beneficial for vacuum quality, since it captures a larger fraction of the primary SR photon fan during the acceleration phase. At lower beam energies the rms vertical aperture of the SR photon fan is bigger, as it depends on the reciprocal of the relativistic factor [103]. The number and position of the pumping slots has been optimised taking into account the leakage of scattered SR power reaching the magnet cold-bore. The internal surface of the beamscreen could be treated using Laser-Ablated Surface Engineering (LASE), creating μm sized patterns on the surface. This treatment has proven [104] to greatly reduce the secondary-electron yield (SEY) of the bare surface. Experimental validation of LASE treated surfaces on the resistive wall impedance to reduce SEY and photo-desorption yield are ongoing in the EC funded EuroCirCol project [104]. Details of the measurements on 3 variations of the beamscreen were reported at the 2018 FCC week [105]. If HTS coatings are chosen for improved impedance reduction, e-cloud mitigation would be provided by an a-C coating.

The HE-LHC dipole magnets are curved. The dipole beamscreens must, therefore, either be produced curved, or be flexible enough that they can be slid into the cold bore of the bent dipole magnets, guided by the sagitta of the magnet.

Future Circular Collider Study
Volume 4 - The High Energy LHC (HE-LHC)
Conceptual Design Report

CONFIDENTIAL DRAFT
V0.7, 3.10.2018
DO NOT DISTRIBUTE

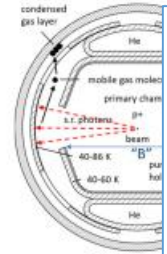

Figure 3.7: Latest design of the
indicated with details of the tempe
width "B" of 27.55 mm. The large
beamscreen of ~860 l/m/s at 50 K
the copper layer on the inside of t
80 µm.

3.3.2.3 *Beamscreen temperature*

The total SR load is ~100 kW/bea
perature between 5 K (inlet) and 2
the corresponding cryo-compressor
than 10 MW [101]. A detailed ana
the beamscreen for a workable sy
outlet of each cell should be betwe
timum working point for a cryoger
resistivity of Cu [107] and also ide
range is also advantageous for the
tional to the square root of the abso
instability is excited [109].

3.3.2.4 *Heat load to cold bore*

Table 3.8 gives an overview of a
mounted using elastic springs in t
results show that the total heat load

Ta

SOURCE
Beam-gas scattering
Thermal conduction
Grey body thermal r
Leaked radiation po
Total heat load

3.3.2.5 *Residual gas density*

The requirements on the residual ga
level was specified for an H_2-equiv

scattering lifetime, i.e. a gas density of a mixture of gases usually released by SR irradiation, consisting of H_2, CO, CO_2, CH_4, each weighted with its radiation length and percentage molecular content and referred to that of 100% H_2 [112]. A scaling has been performed for a hadron beam of higher energy [106]. Given the higher beam energy of HE-LHC and the less-than-linear increase of the nuclear scattering cross-section with beam energy, it has been estimated that a factor of ~2 decrease of the H_2-equivalent density will assure the same 100 hour lifetime contribution as for the LHC. The target is to remain below 5×10^{14} H_2-equivalent m^{-3}.

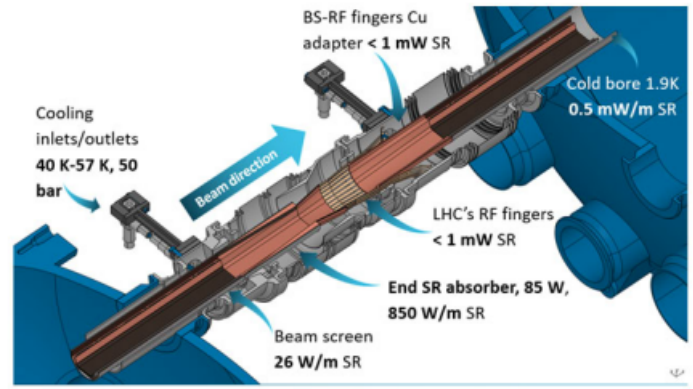

Figure 3.8: Cut-through, in the plane of the orbit, of the dipole-to-dipole short interconnect area model. This model does not show the BPM block, which is under design in another work package.

A 3D CAD model of the arc dipole and interconnect area has been created [112] based on the LHC. It takes into account the new requirements, SR photon flux and linear power densities. It has been found that the RF fingers installed after each dipole and quadrupole, compensating displacements and thermal contraction during cool-down, need to be shielded from the primary SR photon fan. Otherwise be damaged as a result of the 5 W/m power density. A symmetric SR absorber upstream of the RF contact fingers, as used in modern light sources, mitigates that risk. The absorber intercepts and concentrates up to 85 W of SR power, casting a shadow downstream for about 2–3 m, up to the subsequent beamscreen. Along the shadowed area, the racetrack shaped beamscreen gradually merges into the circular shape which is needed for the LHC-style RF contact fingers and, eventually, for the beam-position monitor (BPM) button blocks.

Figure 3.8 shows a cut-away view of the interconnect area. Figure 3.9 shows a residual gas density profile generated by the SR fan after a conditioning time. At each point along the beamscreen, the molecular desorption rate depends on the locally accumulated photon dose. This means that one always has to specify for which photon dose a pressure or density profile is being calculated. The photon dose at each point along the beamscreen is calculated using 3D ray-tracing Monte Carlo simulation that has been validated with experimental data [112].

3.3.2.6 *Electron cloud mitigation*

There are a number of different proposals for electron cloud mitigation. One path currently being considered is using amorphous carbon (aC) coating, which has been successfully tested in the SPS at CERN. Another option is LASE treatment (see Fig. 3.7), which is also being assessed experimentally. Figure 3.10 shows the areas which would need to be treated, the corresponding percentage of copper-coated beamscreen area and the electron cloud distribution for each type of magnetic element: dipole, quadrupole and field-free drift [113].

Future Circular Collider Study
Volume 4 - The High Energy LHC (HE-LHC)
Conceptual Design Report

CONFIDENTIAL DRAFT
V0.7, 3.10.2018
DO NOT DISTRIBUTE

3.3.3.2 Helium absorbers

The absorber material, its shape and its assembly in the cryostat are under investigation. The current conceptual design is based on compacted nano-porous materials fixed in thermal contact with the cold-mass support cooling pipes at 4.5 K (the C' line in LHC terminology).

The development of the He absorbers can benefit from the large spectrum of studies performed over the last ten years, in particular for the ITER project [102, 107, 112]. He pumping has been measured for activated charcoal fixed on metallic surfaces. Surface areas available for absorption regularly exceed 3000 m^2 per gram of absorber; this means that 30 g of activated charcoal would have the same surface area available as the total multi-layer insulation (MLI) in a 400-m long vacuum sector. In the coming years, the focus will be to develop a material with a well defined porous structure for He pumping at affordable cost for quantities around ~100 kg. The activation of the absorbers in the cryostats is also currently under investigation.

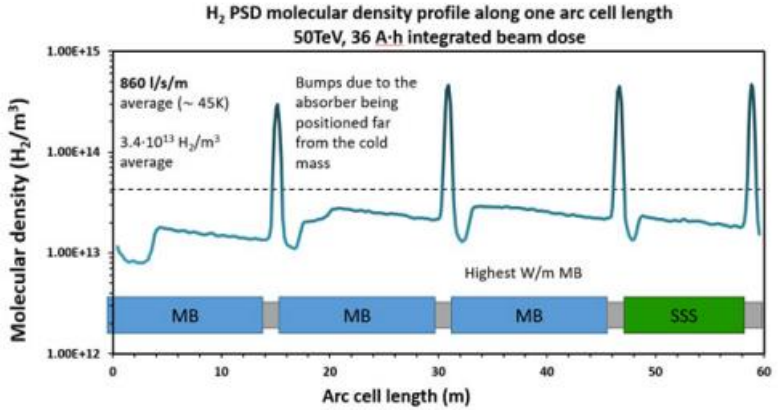

Figure 3.9: H_2 partial pressure profile for one full arc cell. All of the H_2 is due to SR, assuming that the static outgassing and the e-cloud contributions are negligible. The density spikes visible in the plot are located at the photon absorber positions, followed by shallow density minima corresponding to the shadowing of the absorbers and reduced photo-desorption.

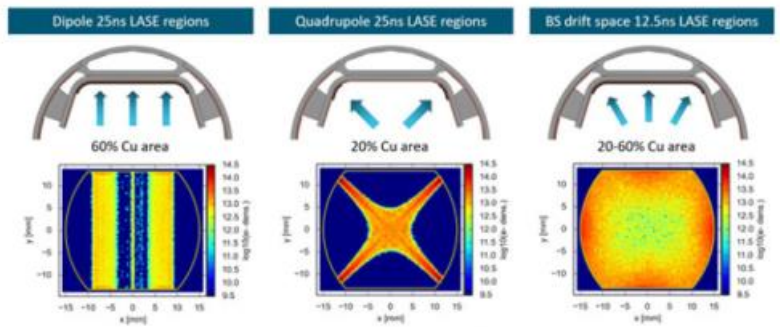

Figure 3.10: Cut-away, of the dipole-to-dipole short interconnect area, in the plane of the orbit. This model does not show the BPM block, which is being designed in another work package.

3.3.3 Vacuum

3.3.3.1 Insulation vacuum design

The insulation vacuum system creates a vacuum barrier between the magnet cryostat and the cryogenic distribution lines. The design will be based on the LHC system [101], which has been operating successfully for more than ten years. By-passes will be possible. Mobile, rough pumping groups will evacuate the large volumes, starting from atmospheric pressure level. Permanent turbo-molecular pumping groups installed at the vacuum barrier by-pass will be used to reach the required target pressure levels and will evacuate helium gas if there are leaks in the cryogenic pipes.

Equipping the arcs with turbo pumps at a spacing comparable to the LHC's appears possible and straightforward. The permanent turbo-molecular groups will also guarantee pumping during thermal transients of the cryostat which lead to excessive gas release from the absorbers.